Superconductivity up to 37.6 K in compressed scandium

Kui Wang,[1,2,*] Yao Sun,[1,2,*] Mi Zhou,[2,*] Hanyu Liu,[1,2,3] Guangchen Ma,[1,2] Hongbo Wang,[1,2,†] Guangtao Liu,[2,‡] and Yanming Ma[1,2,3,§]

[1]*State Key Laboratory of Superhard Materials, College of Physics, Jilin University, Changchun 130012, China*
[2]*Key Laboratory of Material Simulation Methods and Software of Ministry of Education, College of Physics, Jilin University, Changchun 130012, China*
[3]*International Center of Future Science, Jilin University, Changchun 130012, China*

(Received 22 July 2023; revised 8 November 2023; accepted 15 November 2023; published 15 December 2023)

The pursuit of elemental superconductors with high critical temperature (T_c) holds immense scientific significance due to their relatively simple material composition, which not only aids in understanding the mechanisms of superconductivity but also facilitates further exploration of high-temperature superconductors in compound materials. Here, we report experimental findings of superconductivity for scandium (Sc) in the pressure range of 64 GPa to 261 GPa. As a result, the highest T_c of 37.6 K observed in Sc-V phase at 243 GPa sets the current record among all elements. An estimate based on the Ginzburg-Landau model gives a zero-temperature upper critical magnetic field of 21.3 T with a coherence length of 39.3 Å. Current-voltage measurements show that the zero-temperature critical current and its density can reach 0.146 A and 70 A mm^{-2} of Sc-IV at 198 GPa, and 0.116 A and 50 A mm^{-2} of Sc-V at 250 GPa, respectively. Further theoretical calculations show that pressure-induced phonon softening plays a key role in increasing T_c upon compression. Our current findings shed light on the understanding of high superconductivity in simple elements and provide insight into exploring high-T_c elemental superconductors and Sc-based superconductors.

DOI: 10.1103/PhysRevResearch.5.043248

I. INTRODUCTION

Elements, as the foundation of material composition, have always played a crucial role in understanding the underlying physical mechanism due to their simple and fundamental nature [1–8]. The quest for elemental superconductors with high critical temperature (T_c) has been a prominent research area in materials science. To date, approximately 30 elements have been identified to exhibit superconductivity at ambient pressure [9–11]. In recent decades, in particular, high pressure was found to serve as a powerful tool for exploring new superconductors and tuning superconductivity since the significantly pressure-induced modification of electronic orbitals and bonding patterns could help create exotic materials that are inaccessible at ambient conditions [10]. As a consequence, over 20 elements that are not superconducting at ambient pressure have been found to be superconductive [9–11], as well as significant increases in T_c for some elemental superconductors under high pressure [12–21].

Currently, the highest recorded T_c in elemental materials is 29 K, which was observed in Ca in 2011 [15]. Despite more than a decade of effort, elemental materials with higher T_c have yet to be discovered. In metals where *s*, *p* electrons dominate the conduction-band properties, such as Zn, Cd, Al, In, Sn, and Pb, T_c generally decreases initially under pressure [22,23] due to pressure-induced electronic band broadening and lattice stiffening [9,24]. On the contrary, in the case of Ca, Ti, V, and Y, the T_c increase over a wide pressure range [15,17–21], which is attributed to the electron transfer from *s* band to *d* band (*s*-*d* transfer) [25–27]. Therefore, it is natural to ask if there is a new elemental superconductor with higher T_c than Ca?

Sc, as the first element of the transition metal and often classified as rare-earth metals, has attracted significant interest [16,24,28–37]. The high-pressure phase transitions of Sc have been explored up to 297 GPa [32]. Unlike the typical phase-transition sequence observed in IIIB group metals [38–42], Sc undergoes Sc-I ($P6_3/mmc$) – Sc-II ($I4/mcm$) – Sc-III (unsolved fully) – Sc-IV (unsolved fully) – Sc-V ($P6_122$) at around 23, 104, 140, and 239 GPa [32,36], respectively. Nevertheless, the experimental studies on the superconductivity of Sc have only been conducted to 123 GPa [16,24]. It is noteworthy that the increase of *d*-band occupancy (N_d) at this pressure exhibits no signs of saturation, suggesting that further compression to facilitate *s*-*d* transfer completion will likely reach a higher T_c [16]. Debessai *et al.* theoretically pointed out that the T_c of Sc may reach values exceeding 30 K at pressure much higher than 2 Mbar when the *s*-*d* transfer is completed by a phenomenological model [16].

In this work, we conducted comprehensive electrical transport measurements to investigate superconductivity of elemental Sc in the pressure range of 64–261 GPa.

*These authors contributed equally to this work.
†whb2477@jlu.edu.cn
‡liuguangtao@jlu.edu.cn
§mym@jlu.edu.cn

Remarkably, we discovered that Sc exhibited the highest T_c of up to 37.6 K at 243 GPa, establishing a new record among elemental superconductors. Our further simulations suggest that pressure-induced phonon softening plays a key role in increasing T_c for Sc upon compression.

II. METHODS

For electrical transport measurements with and without a magnetic field, we utilize beryllium copper diamond anvil cell (DAC) and steel DACs, respectively. Depending on the desired experimental pressure, we use diamond anvil culets with different sizes. The pertinent information on the used cells is described in Table S1 of the Supplemental Material [43]. All the data presented in the paper were measured during the warming process. In each experiment, we initially compressed the Re gasket with a thickness of 250 μm to approximately 20 GPa pressure. Then we drilled out the bottom of the indentation and filled it with a mixture of aluminum oxide and epoxy. This mixture was subsequently compressed between the anvils to create an insulating layer, which was used to separate the metallic gasket from the Pt electrodes in the electrical measurements. The sample Sc with a purity of 99.9% was purchased from Alfa Aesar. The sample was compressed into a foil with a thickness of 5–11 μm and subsequently loaded into the chamber of the DAC. To prevent the reaction of Sc with air and water, sample preparation and loading were undertaken in an argon-gas glove box with oxygen and water contents below 0.01 ppm. The pressure was measured from the edge of the Raman signal from diamond pressure scale [44]. The electrode configuration and the sample assembly for four-probe Van der Pauw method [45] are illustrated in Fig. S1 of the Supplemental Material [43]. The current used in all resistance measurements was in the range of 10^{-4} to 10^{-3} A, which did not appear to have any discernible impact on T_c. The magnetic field is perpendicular to the sample surface.

The structure relaxations were performed using the density functional theory within the Perdew-Burke-Ernzerhof (PBE) [46] generalized gradient approximation exchange-correlation functional as implemented in the VASP code [47]. The all-electron projector-augmented wave (PAW) [48] method was adopted. Plane wave kinetic energy cutoff was set to 800 eV and Monkhorst-Pack k-meshes [49] with grid spacing of $2\pi \times 0.20$ Å were then adopted to ensure the enthalpy converges well. The electron-phonon coupling (EPC) constant was calculated within the framework of the linear-response theory as carried out in the quantum ESPRESSO package [50]. Ultra-soft pseudopotentials were used with a kinetic energy cutoff of 60 Ry. To calculate the EPC in this system, $6 \times 6 \times 2$ q meshes are utilized for Sc-V and $3 \times 3 \times 3$ q meshes for Sc-III and Sc-IV. The Gaussian broadening is 0.035 Ry for all structures. The T_c was reasonably estimated by the Allen-Dynes modified McMillan equation [7] with the EPC parameter λ below 1.5:

$$T_c = \frac{\omega_{\log}}{1.20} \exp\left[\frac{-1.04(1+\lambda)}{\lambda - \mu^*(1+0.62\lambda)}\right], \qquad (1)$$

where parameters μ^* and $\omega_{\log}$ are the Coulomb pseudopotential and logarithmic average frequency, respectively, which could be numerically calculated by the quantum ESPRESSO package.

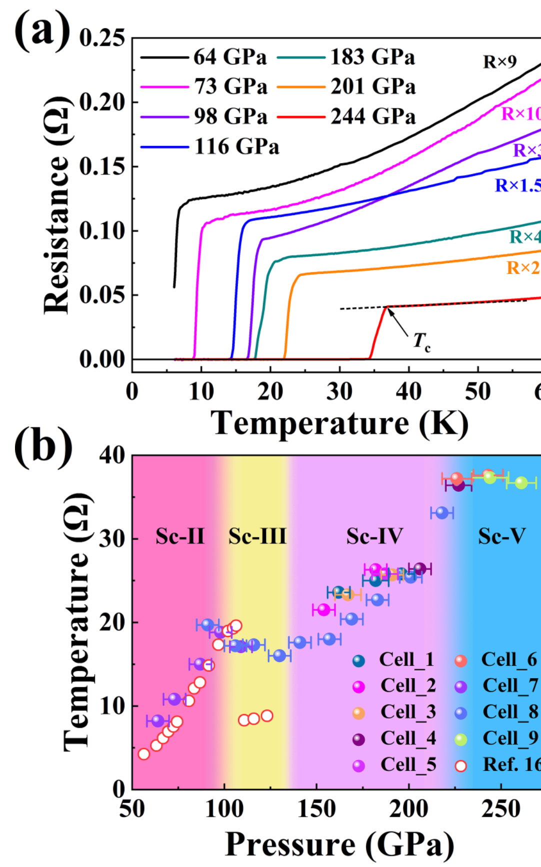

FIG. 1. Superconductivity of Sc metal under high pressure. (a) Representative resistance curves as a function of temperature at typical pressures. The dashed line extending from the normal state on the resistance curve at 244 GPa represents the method for defining the T_c. The curves from 64 GPa to 98 GPa, 116 GPa to 201 GPa, and 244 GPa are from cell_7, cell_8, and cell_9, respectively. For clarity, the resistance of samples at some pressure points was multiplied by the coefficients and annotated with corresponding color. At the low-temperature limit of the experiment, the resistance dropped to zero except for the data of 64 GPa. (b) The T_c as a function of pressure for Sc up to 261 GPa. The results measured in different cells are indicated by solid dots of varying colors. The data represented by the hollow dots are sourced from Ref. [16]. The phase boundaries determined by the T_c are depicted by four color regions: red, yellow, purple, and blue. The error bars represent the uncertainty arising from the pressure gradient on the sample and the pressure determination method.

III. RESULTS AND DISCUSSION

In this work, we prepared 11 cells loaded with precompressed Sc foil as the precursor, designated as cell_1 to cell 11. Using electrical transport measurements, we conducted a comprehensive investigation of the superconducting behavior in phases II to V. Figure 1(a) illustrates several representative R-T curves measured at typical pressures, where the resistance exhibits a sharp drop to zero at low temperature, indicating the occurrence of a superconducting transition. The T_c is defined as the temperature at which the resistance curve starts to deviate from the straight dashed line extrapolated from the normal state as shown in the R-T curve at 244 GPa. The surprising discovery is that as the pressure increased from 64 GPa to 244 GPa, the T_c rose from 8.2 K to 37.3 K, surpassing the current superconductivity record of 29 K held by Ca [15]. To determine the highest value of T_c, we established its dependence on pressure in Sc over a wide range of pressures as shown in Fig. 1(b) (additional data are reported in Fig. S2 of the Supplemental Material [43]). The boundaries of phase transitions were established by identifying significant changes in the T_c with respect to pressure. Superconductivity emerges in the Sc-II phase, with T_c exhibiting a nearly linear increase from 8.2 K at 64 GPa to 18.8 K at 98 GPa, consistent with previous research [16]. At higher pressure conditions, Sc undergoes a transition to the III phase, where T_c gradually decreases with increasing pressure. The observed T_c values are higher than those reported in the literature [16]. This is attributed to the broad drop in the AC susceptibility, where T_c was defined as the midpoint of the drop. Consequently, this approach led to an underestimation of the actual transition temperature. Thus far, the superconducting properties of the Sc-IV and Sc-V phases have not been investigated. After the transition to the Sc-IV phase, the T_c exhibits a steady increase with increasing pressure. However, at approximately 210 GPa, there is a rapid acceleration in the rate of T_c increase, indicating the transition from phase IV to V. Eventually, at around 240 GPa, T_c reaches its maximum value of 37.6 K. Further compression to 261 GPa, the T_c gradually decreases indicating Sc transform into V phase. The phase boundaries determined by T_c are demarcated by the differently colored regions in Fig. 1(b), which shows some deviations from the previous XRD experimental results [32], probably due to the discrepancy in pressure calibration by different methods.

The Meissner effect serves as another independent criterion necessary for confirming superconductivity. However, the measurement of weak magnetic signals from a 20-micron sample inside a diamond anvil cell is widely acknowledged as a challenging task [51]. An applied external field could break the Cooper pairs due to the Pauli paramagnetic effect of electron spin polarization and the diamagnetic effect of the orbital motion, thus reducing the value of T_c. Consequently, the suppression of T_c by external magnetic fields is an alternative approach to validate the nature of the superconducting transition. Therefore, we conducted electrical transport measurements under different magnetic fields at 241 GPa to further investigate the superconductivity of Sc under high pressures. Figure 2 shows that the application of a magnetic field $\mu_0 H = 9$ T effectively reduces T_c by approximately 9.1 K, thereby confirming the superconducting transition. The extrapolation value of the upper critical field $\mu_0 H$ toward $T = 0$ K is 21.3 T fitted by the Ginzburg-Landau (GL) [52] models $\mu_0 H_{c2}(T) = \mu_0 H_{c2}(0)[1 - (T/T_c)^2]$. The GL coherence length was calculated to be $\xi = 39.3$ Å via $\xi = [h/(4\pi e H_{c2})]^{\frac{1}{2}}$ [53].

Another distinguishing feature of superconductors is the existence of an upper critical current density (J_c) at which superconductivity disappears. The critical currents for the Sc-IV and Sc-V phases, which have not been experimentally studied for superconductivity before, were investigated in the current range of 10^{-5} to 10^{-1} A under external magnetic fields as shown in Figs. 3 and S3. It can be seen that the critical current value decreases with rising temperature and magnetic field, thereby providing additional evidence of its superconductivity. The estimate of the critical (J_c) is based on the fact that the sample will not exceed the culet size (30 μm) and the thickness is less than the thickness of the initial sample (7 μm). Figure 3 shows the critical current fitting curve at different magnetic fields (including zero magnetic fields) using the formula $J_c(T) = J_c(0)[1 - (T/T_c)^2]$. At zero field, the extrapolation value of the upper critical current toward $T = 0$ K of the Sc-IV and Sc-V phases can reach 0.146 A and 0.116 A, respectively, and values of the density are approximately 70 A mm^{-2} and 50 A mm^{-2}. It is worth mentioning that we have overestimated the cross-sectional area of the sample, so the actual $J_c(0)$ is greater than these values.

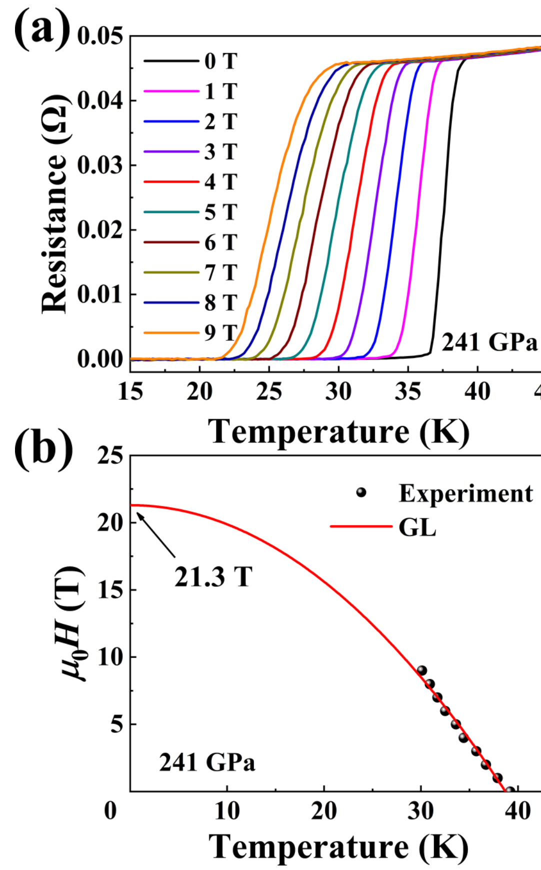

FIG. 2. Superconducting transition of compressed Sc metal under external magnetic fields. (a) Temperature dependence of the resistance of Sc metal under applied magnetic fields of up to 9 T at 241 GPa. (b) The upper critical fields $\mu_0 H_c$ extrapolated to the limit of zero temperature at 241 GPa. The experimental data points are fitted with the formalism of the GL model.

Given that the previous research [16] has indicated the primary role of s-d transfer in enhancing T_c for transition metal elements like Sc, we also investigated the N_d and d electron density of states under high pressure. With increasing pressure, the N_d value continues to rise in accordance with the previous results [16], however, the contribution of d electrons at the Fermi level remains relatively constant despite it has always dominated (Fig. S4 [43]). Therefore, the increase of

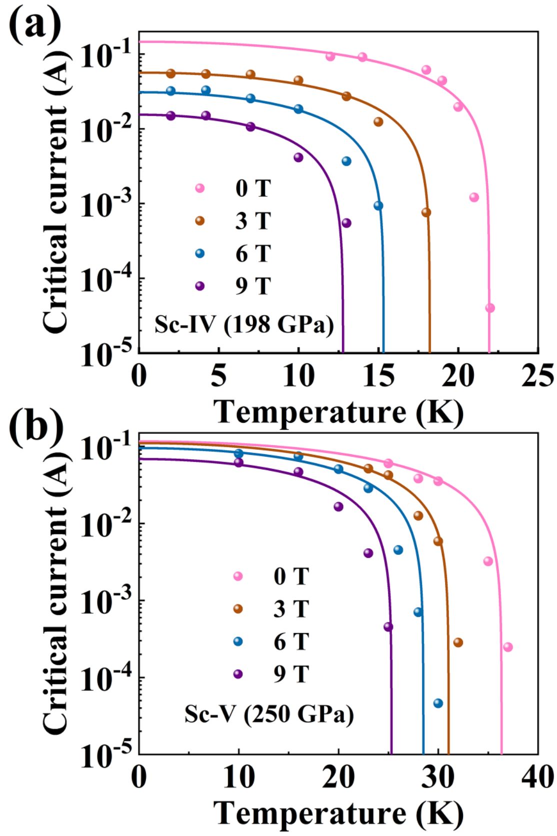

FIG. 3. The critical current measurement of Sc-IV and Sc-V phases. (a), (b) Extrapolation of the temperature dependence of critical current at different magnetic fields of Sc-IV at 198 GPa and Sc-V at 250 GPa. The dots are the experimental data, and the curves are plotted by fitting the formula $J_c(\mathrm{T}) = J_c(0)[1\text{-}(T/T_c)^2]$.

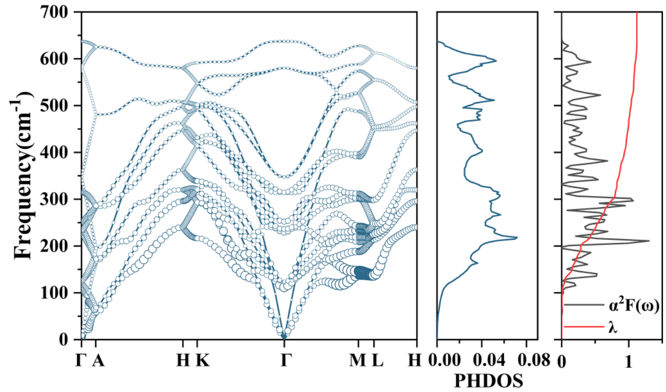

FIG. 4. Electronic properties of Sc-V at 260 GPa. Calculated phonon dispersion curves (hollow circle proportional to associated EPC), projected phonon density of states (PHDOS), and Eliashberg phonon function $\alpha^2\mathrm{F}(\omega)$ and its integral $\lambda(\omega)$ of Sc-V at 260 GPa.

N_d cannot be responsible for the enhanced T_c in elemental Sc. In fact, the *s*-*d* electron transfer is common in transition metals under high pressures [25,27,54], because the energy of the *s* band will be significantly increased compared with the *d* band [55].

To elucidate the high T_c observed in compressed Sc metal, we perform subsequent calculations to investigate the trend of T_c for Sc upon compression and the origin of high T_c at high pressure. The superconducting parameters including their EPC constant λ, the logarithmic average frequency ($\omega_{\log}$), as well as the T_cs obtained by Allen-Dynes modified McMillan (MAD) [7] formula of Sc-III, Sc-IV, Sc-V are shown in Table I. It is clearly seen that the T_cs of Sc increase with pressure, which is consistent with the results of experiments. In Fig. 4, we find substantial phonon softening in Γ point at 260 GPa for Sc-V. The same phenomenon is also found in the Γ point in Sc-III and Z to T and R to Z directions in Sc-IV (Fig. S5 [43]). For Sc-V, the improvement of λ and $\omega_{\log}$ show that pressure-induced phonon softening and the increase in the frequency of interatomic vibrations make the T_c of Sc-V exceed 30 K. On the basis, pressure-induced phonon softening plays a key role in increasing λ as well as T_c for Sc upon compression.

IV. CONCLUSIONS

In summary, we have reported a superconducting record in elemental superconductors, achieving a T_c of 37.6 K at 243 GPa in Sc. Theoretical calculations indicate that the increase in T_c is primarily attributed to phonon softening induced by high pressure. These findings offer a fresh perspective on the superconducting mechanism of transition metal elements, which holds significant importance for the design and synthesis of high-T_c Sc-based superconductors.

Note added. During the preparation of our manuscript, we became aware that similar results on T_c enhancement in highly compressed Sc metal were independently obtained by two other groups [56,57].

ACKNOWLEDGMENTS

This work was supported by the National Natural Science Foundation of China (Grant Nos. 52288102, 52090024, 12374007, 12074139, and 12074138) and the Strategic Priority Research Program of Chinese Academy of Sciences (Grant No. XDB33000000).

TABLE I. The calculated superconducting parameters of Sc-III, Sc-IV, and Sc-V.

				States/eV/atom				T_c(K)	
Compounds	Pressure (GPa)	λ	$\omega_{\log}$ (K)	s	p	d	N_{Ef}	$\mu^* = 0.10$	$\mu^* = 0.13$
Sc-III	100	0.79	261	0.017	0.034	0.356	0.411	11.9	9.6
Sc-IV	170	1.11	264	0.033	0.039	0.322	0.397	21.5	18.8
Sc-V	260	1.12	367	0.023	0.039	0.369	0.439	30.1	26.4

[1] H. K. Onnes, The resistance of pure mercury at helium temperature, Commun. Phys. Lab. Univ. Leiden. **120b**, 261 (1911).

[2] R. Wang and M. D. Merz, Non-crystallinity and polymorphism in elemental solids, Nature (London) **260**, 35 (1976).

[3] L. Lu, Y. Shen, X. Chen, L. Qian, and K. Lu, Ultrahigh strength and high electrical conductivity in copper, Science **304**, 422 (2004).

[4] O. Prakash, A. Kumar, A. Thamizhavel, and S. Ramakrishnan, Evidence for bulk superconductivity in pure bismuth single crystals at ambient pressure, Science **355**, 52 (2017).

[5] S. Jiang *et al.*, Ultrastrong steel via minimal lattice misfit and high-density nanoprecipitation, Nature (London) **544**, 460 (2017).

[6] W. L. McMillan, Transition temperature of strong-coupled superconductors, Phys. Rev. **167**, 331 (1968).

[7] P. B. Allen and R. C. Dynes, Transition temperature of strong-coupled superconductors reanalyzed, Phys. Rev. B **12**, 905 (1975).

[8] M. Kawamura, Y. Hizume, and T. Ozaki, Benchmark of density functional theory for superconductors in elemental materials, Phys. Rev. B **101**, 134511 (2020).

[9] J. J. Hamlin, Superconductivity in the metallic elements at high pressures, Physica C **514**, 59 (2015).

[10] L. Zhang, Y. Wang, J. Lv, and Y. Ma, Materials discovery at high pressures, Nat. Rev. Mater. **2**, 17005 (2017).

[11] K. Shimizu, Superconducting elements under high pressure, Physica C **552**, 30 (2018).

[12] K. Shimizu, H. Ishikawa, D. Takao, T. Yagi, and K. Amaya, Superconductivity in compressed lithium at 20 K, Nature (London) **419**, 597 (2002).

[13] V. V. Struzhkin, M. I. Eremets, W. Gan, H. Mao, and R. J. Hemley, Superconductivity in dense lithium, Science **298**, 1213 (2002).

[14] V. V. Struzhkin, R. J. Hemley, H. Mao, and Y. A. Timofeev, Superconductivity at 10–17 K in compressed sulphur, Nature (London) **390**, 382 (1997).

[15] M. Sakata, Y. Nakamoto, K. Shimizu, T. Matsuoka, and Y. Ohishi, Superconducting state of Ca-VII below a critical temperature of 29 K at a pressure of 216 GPa, Phys. Rev. B **83**, 220512(R) (2011).

[16] M. Debessai, J. J. Hamlin, and J. S. Schilling, Comparison of the pressure dependences of T_c in the trivalent *d*-electron superconductors Sc, Y, La, and Lu up to megabar pressures, Phys. Rev. B **78**, 064519 (2008).

[17] X. Liu, P. Jiang, Y. Wang, M. Li, N. Li, Q. Zhang, Y. Wang, Y.-L. Li, and W. Yang, T_c up to 23.6 K and robust superconductivity in the transition metal δ-Ti phase at megabar pressure, Phys. Rev. B **105**, 224511 (2022).

[18] C. Zhang, *et al.*, Record high T_c element superconductivity achieved in titanium, Nat. Commun. **13**, 5411 (2022).

[19] K. Wang, C. Liu, G. Liu, X. Yu, M. Zhou, H. Wang, C. Chen, and Y. Ma, Evidence for an emergent anomalous metallic state in compressed titanium, Proc. Natl. Acad. Sci. USA **120**, e2218856120 (2023).

[20] M. Ishizuka, M. Iketani, and S. Endo, Pressure effect on superconductivity of vanadium at megabar pressures, Phys. Rev. B **61**, R3823(R) (2000).

[21] J. J. Hamlin, V. G. Tissen, and J. S. Schilling, Superconductivity at 20 K in yttrium metal at pressures exceeding 1 Mbar, Physica C **451**, 82 (2007).

[22] C. Buzea and K. Robbie, Assembling the puzzle of superconducting elements: A review, Supercond. Sci. Technol. **18**, R1 (2005).

[23] J. S. Schilling, Superconductivity in the alkali metals, High Press. Res. **26**, 145 (2006).

[24] J. J. Hamlin and J. S. Schilling, Pressure-induced superconductivity in Sc to 74 GPa, Phys. Rev. B **76**, 012505 (2007).

[25] H. L. Skriver, Crystal structure from one-electron theory, Phys. Rev. B **31**, 1909 (1985).

[26] A. K. McMahan, Pressure-induced changes in the electronic structure of solids, Physica B+C **139–140**, 31 (1986).

[27] D. G. Pettifor, Theory of energy bands and related properties of 4d transition metals. I. Band parameters and their volume dependence, J. Phys. F **7**, 613 (1977).

[28] A. Ormeci, K. Koepernik, and H. Rosner, First-principles electronic structure study of Sc-II, Phys. Rev. B **74**, 104119 (2006).

[29] L. W. Nixon, D. A. Papaconstantopoulos, and M. J. Mehl, Calculations of the superconducting properties of scandium under high pressure, Phys. Rev. B **76**, 134512 (2007).

[30] S. K. Bose, Linear response results for phonons and electron–phonon coupling in hexagonal close packed Sc-spin fluctuations, and implications for superconductivity, J. Phys.: Condens. Matter **20**, 045209 (2008).

[31] Y. C. Zhao, F. Porsch, and W. B. Holzapfel, Evidence for the occurrence of a prototype structure in Sc under pressure, Phys. Rev. B **54**, 9715 (1996).

[32] Y. Akahama, H. Fujihisa, and H. Kawamura, New helical chain structure for scandium at 240 GPa, Phys. Rev. Lett. **94**, 195503 (2005).

[33] S. Arapan, N. V. Skorodumova, and R. Ahuja, Determination of the structural parameters of an incommensurate phase from first principles: The case of Sc-II, Phys. Rev. Lett. **102**, 085701 (2009).

[34] B. Kong, L. Zhang, X.-R. Chen, T.-X. Zeng, Z.-Y. Zeng, and L.-C. Cai, From first principles: Phase transition mechanisms of hexagonal Sc and Y under pressure, Solid State Commun. **151**, 1972 (2011).

[35] R. Briggs, M. G. Gorman, A. L. Coleman, R. S. McWilliams, E. E. McBride, D. McGonegle, J. S. Wark, L. Peacock, S. Rothman, S. G. Macleod *et al.*, Ultrafast x-ray diffraction studies of the phase transitions and equation of state of scandium shock compressed to 82 GPa, Phys. Rev. Lett. **118**, 025501 (2017).

[36] S-C. Zhu, X-Z. Yan, S. Fredericks, Y-L. Li, and Q. Zhu, First-principles investigation of Sc-III/IV under high pressure, Phys. Rev. B **98**, 214116 (2018).

[37] W. A. Grosshans, Y. K. Vohra, and W. B. Holzapfel, High pressure phase transformations in yttrium and scandium: Relation to rare earths and actinides crystal structures, J. Magn. Magn. Mater. **29**, 282 (1982).

[38] B. Johansson and A. Rosengren, Generalized phase diagram for the rare-earth elements: Calculations and correlations of bulk properties, Phys. Rev. B **11**, 2836 (1975).

[39] Y. K. Vohra, H. Olijnik, W. Grosshans, and W. B. Holzapfel, Structural phase transitions in yttrium under pressure, Phys. Rev. Lett. **47**, 1065 (1981).

[40] Y. K. Vohra, V. Vijayakumar, B. K. Godwal, and S. K. Sikka, Structure of the distorted fcc high-pressure phase of the trivalent rare-earth metals, Phys. Rev. B **30**, 6205(R) (1984).

[41] F. Porsch and W. B. Holzapfel, Novel reentrant high pressure phase transition in lanthanum, Phys. Rev. Lett. **70**, 4087 (1993).

[42] N. Hamaya, Y. Sakamoto, H. Fujihisa, Y. Fujii, K. Takemura, T. Kikegawa, and O. Shimomura, Crystal structure of the distorted FCC high-pressure phase of praseodymium, J. Phys.: Condens. Matter **5**, L369 (1993).

[43] See Supplemental Material at http://link.aps.org/supplemental/10.1103/PhysRevResearch.5.043248 for details of sample preparation, all the electrical resistance curves, the results of critical current measurement, and calculated results of electronic properties.

[44] Y. Akahama and H. Kawamura, Pressure calibration of diamond anvil Raman gauge to 310 GPa, J. Appl. Phys. **100**, 043516 (2006).

[45] L. J. van der Pauw, A method of measuring specific resistivity and Hall effect of discs of arbitrary shape, Philips Res. Rep. **13**, 1 (1958).

[46] J. P. Perdew, K. Burke, and M. Ernzerhof, Generalized gradient approximation made simple, Phys. Rev. Lett. **77**, 3865 (1996).

[47] G. Kresse and J. Furthmüller, Efficient iterative schemes for *ab initio* total-energy calculations using a plane-wave basis set, Phys. Rev. B **54**, 11169 (1996).

[48] P. E. Blöchl, Projector augmented-wave method, Phys. Rev. B **50**, 17953 (1994).

[49] H. J. Monkhorst and J. D. Pack, Special points for Brillouin-zone integrations, Phys. Rev. B **13**, 5188 (1976).

[50] P. Giannozzi *et al.*, QUANTUM ESPRESSO: A modular and open-source software project for quantum simulations of materials, J. Phys.: Condens. Matter **21**, 395502 (2009).

[51] A. P. Drozdov *et al.*, Superconductivity at 250 K in lanthanum hydride under high pressures, Nature (London) **569**, 528 (2019).

[52] V. L. Ginzburg and L. D. Landau, On the theory of superconductivity, Zh. Eksp. Teor. Fiz. **20**, 1064 (1950).

[53] M. Tinkham, *Introduction to Superconductivity* 2nd ed. (McGraw-Hill, New York, 1996).

[54] J. C. Duthie and D. G. Pettifor, Correlation between *d*-band occupancy and crystal structure in the rare earths, Phys. Rev. Lett. **38**, 564 (1977).

[55] Y. K. Vohra and P. T. Spencer, Novel γ-phase of titanium metal at megabar pressures, Phys. Rev. Lett. **86**, 3068 (2001).

[56] J. Ying, S. Liu, Q. Lu, X. Wen, Z. Gui, Y. Zhang, X. Wang, J. Sun, and X. Chen, Record high 36 K transition temperature to the superconducting state of elemental scandium at a pressure of 260 GPa, Phys. Rev. Lett. **130**, 256002 (2023).

[57] X. He *et al.*, Superconductivity above 30 K achieved in dense scandium, Chinese Phys. Lett. **40** 107403 (2023).